

Double dissociation of structure-function relationships in memory and fluid intelligence observed with magnetic resonance elastography

Curtis L. Johnson^{a,*}, Hillary Schwarb^{b,*}, Kevin M. Horecka^b, Matthew D.J. McGarry^c, Charles H. Hillman^{d,e}, Arthur F. Kramer^{b,d}, Neal J. Cohen^b, Aron K. Barbey^{b,*}

^a Department of Biomedical Engineering, University of Delaware, Newark, DE, United States

^b Beckman Institute for Advanced Science and Technology, University of Illinois at Urbana-Champaign, Urbana, IL, United States

^c Department of Biomedical Engineering, Columbia University, New York, NY, United States

^d Department of Psychology, Northeastern University, Boston, MA, United States

^e Department of Health Sciences, Northeastern University, Boston, MA, United States

ARTICLE INFO

Keywords:

Magnetic resonance elastography

Relational memory

Fluid intelligence

Hippocampus

Orbitofrontal cortex

ABSTRACT

Brain tissue mechanical properties, measured *in vivo* with magnetic resonance elastography (MRE), have proven to be sensitive metrics of neural tissue integrity. Recently, our group has reported on the positive relationship between viscoelasticity of the hippocampus and performance on a relational memory task in healthy young adults, which highlighted the potential of sensitive MRE measures for studying brain health and its relation to cognitive function; however, structure-function relationships outside of the hippocampus have not yet been explored. In this study, we examined the relationships between viscoelasticity of both the hippocampus and the orbitofrontal cortex and performance on behavioral assessments of relational memory and fluid intelligence. In a sample of healthy, young adults ($N = 53$), there was a significant, positive relationship between orbitofrontal cortex viscoelasticity and fluid intelligence performance ($r = 0.42$; $p = .002$). This finding is consistent with the previously reported relationship between hippocampal viscoelasticity and relational memory performance ($r = 0.41$; $p = .002$). Further, a significant double dissociation between the orbitofrontal-fluid intelligence relationship and the hippocampal-relational memory relationship was observed. These data support the specificity of regional brain MRE measures in support of separable cognitive functions. This report of a structure-function relationship observed with MRE beyond the hippocampus suggests a future role for MRE as a sensitive neuroimaging technique for brain mapping.

Introduction

Measuring the *in vivo* mechanical properties of the human brain with magnetic resonance elastography (MRE) (Muthupillai et al., 1995) has recently found clinical applications in radiology, neurology, and neurosurgery (Hiscox et al., 2016; Johnson and Telzer, 2017). MRE studies have revealed softening of neural tissue in several neurological disorders associated with neurodegeneration (Huston et al., 2016; Murphy et al., 2016; Romano et al., 2014; Streitberger et al., 2012), and the assessment of intracranial tumor stiffness has shown promise in surgical planning (Hughes et al., 2015; Hughes et al., 2016). Part of the success of MRE is owed to the high sensitivity of mechanical properties to microstructural tissue health; indeed, viscoelastic parameters relate to tissue composition and organization (Sack et al., 2013) and compositional and

organizational changes accompanying viscoelastic property changes have been observed in animal models of demyelination (Schregel et al., 2012), inflammation (Riek et al., 2012), and neuronal loss (Freimann et al., 2013). Beyond disease, MRE has also revealed differences in viscoelasticity in the healthy aging brain (Arani et al., 2015; Sack et al., 2011), presumably reflecting natural changes in brain health.

The high sensitivity of brain tissue viscoelasticity to microstructure has also motivated its use in answering cognitive neuroscience questions about structure-function relationships, as it is well documented that across the brain, the health and integrity of the underlying tissue can influence cognitive function and success (Raz, 2000). Our group has recently reported a positive relationship between the relative viscosity of the hippocampus (HC) measured with MRE and relational memory performance assessed with a spatial reconstruction (SR) task (Schwarb et

* Corresponding authors.

E-mail addresses: clj@udel.edu (C.L. Johnson), schwarb2@illinois.edu (H. Schwarb), barbey@illinois.edu (A.K. Barbey).

¹ Equal contribution.

al., 2016). We have also observed that the HC viscoelasticity measured from MRE appears to convey the benefits of aerobic fitness and exercise training on memory performance (Sandroff et al., 2017; Schwarb et al., 2017). Taken together, these studies highlight an exciting new role for MRE that harnesses its inherent sensitivity to tissue microstructure to explore structure-function relationships in the brain; however, to date, HC structure-function relationships remain the only such relationships explored with MRE. This is in part due to the challenges associated with localizing MRE property measures to specific regions of cortical gray matter due to its very thin structure and sulcal discontinuities. Overcoming these limitations requires high resolution imaging and mechanical inversion techniques (Johnson et al., 2013b; Johnson et al., 2016), and we hypothesized that, by adopting a high-resolution MRE scheme for assessing the cortex, we could observe other structure-function relationships with MRE.

We tested this by examining the viscoelasticity of the orbitofrontal cortex (OFC) and its relationship with fluid intelligence performance assessed with a figure series (FS) task (Cattell, 1971; Daugherty et al., 2018). Fluid intelligence is the ability (Carroll, 1993; Cattell, 1971) that supports flexible, abstract, and adaptive thinking (Barbey et al., 2013; de Abreu et al., 2010; Jaeggi et al., 2008; Masunaga et al., 2008). Traditionally, damage to the prefrontal cortex (PFC) generally has resulted in impairment on tasks designed to measure fluid intelligence (Barbey et al., 2013; Duncan et al., 1995; Woolgar et al., 2010). Of course, the PFC is a large, non-homogeneous region comprising many structurally and functionally differentiated subregions, including the lateral PFC, anterior cingulate cortex, and OFC, which have been identified as particularly important for fluid intelligence (Barbey et al., 2013; Woolgar et al., 2010; but see Tranel et al., 2008). Different measures of fluid intelligence also engage different PFC regions. Functional neuroimaging studies of canonical FS reasoning tasks of fluid intelligence (e.g. the Cattell Culture Fair task; CCF) engage middle frontal gyrus and OFC (Duncan et al., 2000; Masunaga et al., 2008). Volumetric studies on older adults have also been informative in localizing PFC contributions to fluid intelligence performance highlighting the role of the OFC. Gong and colleagues reported that after controlling for the effects of age, volume in the medial PFC extending into the OFC correlated with performance on a figure series task (Gong et al., 2005). Raz and colleagues corroborated and further refined these findings, and demonstrated that, after controlling for age, sex, and vascular risk factors, OFC volume specifically predicted performance on the CCF task (Raz et al., 2008). Based on these previous findings, the current experiment focused on OFC viscoelasticity and figure series task measures to explore its relationship with fluid intelligence.

Further, we hypothesized that observed structure-function relationships dissociate with each other. We therefore compared the OFC-fluid intelligence relationship with the previously-established HC-relational memory relationship. The hippocampus is critically involved in relational memory abilities (Cohen and Eichenbaum, 1993; Eichenbaum and Cohen, 2001) and we have previously shown that MRE derived measures of HC viscoelasticity are sensitive to relational memory success among healthy young adults (Schwarb et al., 2016; Schwarb et al., 2017). Derived primarily from behavioral and lesion studies, the gold standard for identifying dissociable and selective structure-function relationships is the double-dissociation (Bigler, 2009; Fama and Sullivan, 2014; Freedman et al., 1984; Teuber, 1955). Generally, a double dissociation necessitates that brain region A relates to or impacts cognitive process X, but not (or to a significantly lesser extent) cognitive process Y; while brain region B relates to or impacts cognitive process Y, but not (or to a significantly lesser extent) cognitive process X. In the current study, we apply this framework to our MRE measures of microstructural integrity predicting that among healthy, young adults, HC viscoelasticity will show a significant relationship with performance on measures of relational memory, but not fluid intelligence; and that OFC viscoelasticity will show a significant relationship with performance on measures of fluid intelligence, but not relational memory. Together, these data

provide the first evidence to support the specificity of structure-function relationships from MRE, and motivates the use of MRE in mechanically mapping the human brain to understand its structure, function, and health.

Methods

Participants

Participants were recruited from the Urbana-Champaign community as part of a larger cognitive training intervention study designed to assess the efficacy of different intervention modalities on cognitive performance in healthy adults ($N = 384$). A small number of participants ($N = 64$) volunteered to complete an optional additional imaging session that included an MRE scan. The University of Illinois Urbana-Champaign Institutional Review Board approved all aspects of the study and participants provided informed consent at enrollment. All participants were right-handed with normal or corrected-to-normal vision without color blindness, reported no previous neurological disorders or surgeries, were not on medications affecting central nervous function, and were not pregnant. Participants received monetary compensation for their participation. Only those participants who completed MRE scans are included in this report. A subsample of this population has previously been reported (Schwarb et al., 2017).

As such, data were collected from 64 participants ages 18–35 (mean age = 22.7) and included 32 males and 32 females. Five participants were excluded as they did not complete the hippocampal-dependent SR memory task. Due to significant skewness in some of our variables of interest, median absolute deviation (MAD) methods were used to detect statistical outliers (Hampel, 1974; Leys et al., 2013). A conservative criterion of 3 times the MAD was used for outlier detection (Miller, 1991). As such, five participants were removed based on their memory performance measures and an additional participant was excluded due to hippocampal MRE viscoelasticity measures. The resulting sample included 53 participants ages 18–35 (mean age = 22.8) and included 26 men and 27 women.

All participants completed a behavioral assessment session and an MRI scanning session. The MRI session was completed on a Siemens 3T Trio scanner with 32-channel head coil (Siemens Medical Solutions; Erlangen, Germany).

MRE acquisition and analysis

We acquired MRE displacement data using a 3D multislabs, multi-shot spiral sequence (Johnson et al., 2014). Imaging parameters included: 2 in-plane, constant density spiral shots ($R = 2$) (Glover, 1999); 1800/73 ms repetition/echo times; 240 mm field-of-view; 150×150 matrix; 60 slices at 1.6 mm thickness (acquired in 10 slabs of 8 slices each with 25% overlap). The final imaging resolution was $1.6 \times 1.6 \times 1.6 \text{ mm}^3$. Images were reconstructed using an iterative algorithm (Sutton et al., 2003) that included parallel imaging with SENSE (Pruessmann et al., 2001), field inhomogeneity correction with an auxiliary field map (Funai et al., 2008), and motion-induced phase error correction (Johnson et al., 2013b; Johnson et al., 2014).

The MRE sequence captured displacements using motion-sensitive gradients synchronized to applied 50 Hz vibrations, which were delivered to the head using a pneumatic actuator with soft pillow driver (Resoundant, Inc.; Rochester, MN). Gradients were applied separately in three directions, with both positive and negative polarity to remove background phase, and with varying synchronization to vibration to sample four time points evenly spaced over one period. The total acquisition time was approximately 12 min. Following image reconstruction and data processing (including phase subtraction, temporal filtering (Manduca et al., 2001), and phase unwrapping (Jenkinson, 2003)), complex, full vector displacement fields were generated for mechanical property estimation.

We used the nonlinear inversion (NLI) algorithm (McGarry et al., 2012) to calculate the mechanical properties in the brain. NLI returns maps of the complex shear modulus, $G = G' + iG''$, from which we compute the shear stiffness (Manduca et al., 2001), $\mu = 2|G|^2/(|G| + G')$, and the damping ratio (McGarry and Van Houten, 2008), $\xi = G''/2G'$. We will further note that, consistent with our previous work, we report the adjusted damping ratio, $\xi' = 1 - \xi$, as a dimensionless parameter that describes the relative elastic-viscous behavior of the viscoelastic tissue. Higher ξ' indicates more elastic behavior, while lower ξ' indicates more viscous behavior.

To improve the calculation of regional properties of the HC and OFC we incorporated *a priori* spatial information using soft prior regularization (SPR) in the NLI formulation (McGarry et al., 2013), as in our previous work investigating the HC with MRE (Sandroff et al., 2017; Schwarb et al., 2016, 2017). SPR uses spatial masks and penalizes variations in recovered properties across those masks, effectively promoting local homogeneity in prescribed regions, and improves sensitivity and repeatability of measurements (Johnson et al., 2016). Subject-specific masks were created through segmentation of a high-resolution T₁-weighted anatomical image ($0.9 \times 0.9 \times 0.9 \text{ mm}^3$ voxel size; 1900/900/2.32 ms repetition/inversion/echo times) using FreeSurfer 5.3 (Desikan et al., 2006; Fischl, 2012; Fischl et al., 2002). Automatic segmentation of the HC, lateral OFC, medial OFC, and pericalcarine cortex (PCC) was performed, as in (Schwarb et al., 2016; Schwarb et al., 2017). All segmentations were visually inspected for accuracy and manual corrections were made when necessary. Parcellated volumes were then converted into regional masks in MRE native space using FLIRT in FSL (Jenkinson et al., 2002; Jenkinson et al., 2012) for incorporation into the NLI routine. Medial and lateral OFC masks were combined to create a single OFC mask, and the PCC is included as a control region. The PCC, a primary visual region, served as an optimal control region as it is typically important for early visual processing, but not differentially involved in tasks of relational memory and fluid intelligence. The MRE analyses and outcome measures are illustrated in Fig. 1 a.

Volume and cortical thickness

Measures of HC volume (Buckner et al., 2004) and OFC and PCC

thickness (Fischl and Dale, 2000) were calculated using FreeSurfer (Fischl, 2012). HC volume was normalized by intracranial volume (ICV) (Erickson et al., 2009; Raz et al., 2005). Mean cortical thickness was included as a co-variate when considering correlations with OFC and PCC thickness (Winkler et al., 2010).

Cognitive performance

Relational memory was assessed using a computerized SR task (Monti et al., 2015; Schwarb et al., 2016, 2017) (Fig. 1b). On each trial, participants studied the location of six abstract line drawings randomly distributed on the screen. Displays were studied for 20 s before stimuli disappeared for 4 s and reappeared in a straight line at the top of the screen. Participants then used the mouse to drag each stimulus back to its studied location. Reconstruction was self-paced and participants were allowed to adjust their reconstruction until they were satisfied that they had recreated the original display. Each assessment included 20 trials. Accuracy was the primary outcome measure, and was calculated by determining if each stimulus was both correctly associated with its target location and accurately placed at that location. Association was determined by computing a global minimal mapping of items to locations without considering stimulus identity (Burkard et al., 2012). If, after adjusting for this minimal mapping, a given stimulus remained associated with its target location, it was identified as correctly associated. Next, to evaluate accuracy, a misplacement distribution across all stimuli was computed on the adjusted data and any stimulus within a 95% confidence interval around its target location was counted as accurate. The total possible accuracy score was six (i.e. the number of stimuli per trial).

Fluid intelligence was assessed using a computerized figure series task (Daugherty et al., 2018) (Fig. 1c). Figure series (FS) is a canonical measure of fluid intelligence in which participants must accurately select the information missing from a series by identifying the organizational rule governing that series (Cattell, 1971; Daugherty et al., 2018). One minute was allotted for each of the 30 trials. Accuracy (the number of correct responses) was the outcome measure. Trials for which the allotted 1 min time limit was exceeded were included as inaccurate responses. The total

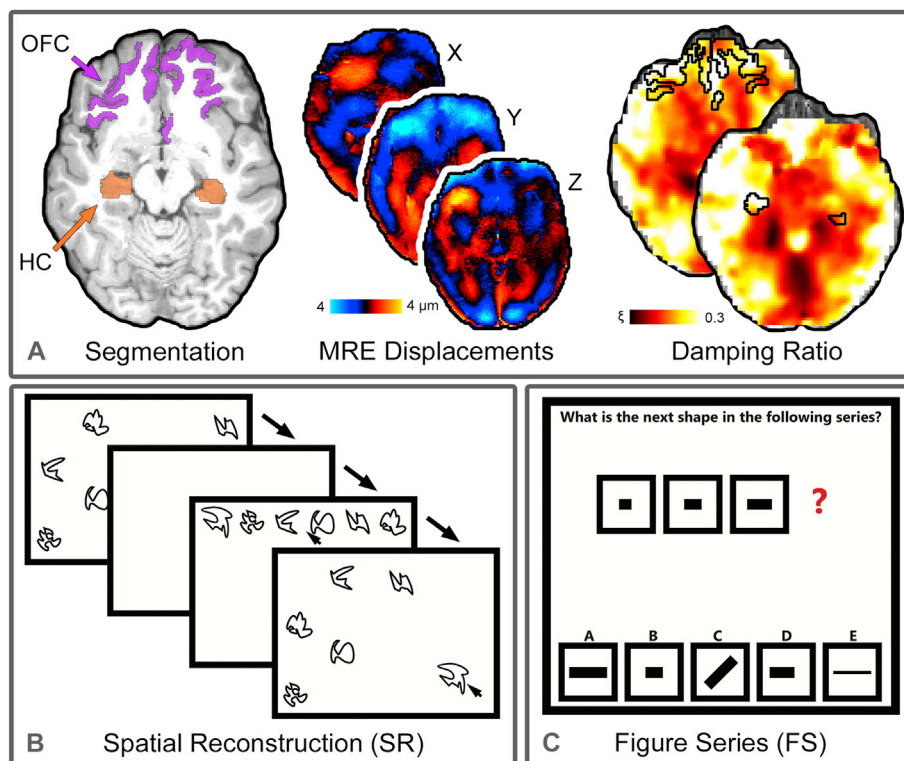


Fig. 1. A) Overview of the elastography procedure. Hippocampal (HC) and orbitofrontal cortex (OFC) structures were automatically segmented from T₁-weighted images using FreeSurfer and converted into masks. Three-dimensional, full vector, complex displacement fields, with 1.6 mm isotropic voxels, were captured via MRE imaging acquisition for mechanical property estimation with nonlinear inversion. Soft prior regularization processes were applied to promote regional homogeneity during estimation and further reduce partial volume effects. The procedure returns tissue viscoelastic properties: shear stiffness, μ , and damping ratio, ξ . B) Illustration of the spatial reconstruction task (SR). On each trial participants studied a display that included six objects. After a short delay, participants used the mouse to reconstruct the display that they had just studied. This provides a measure of relational memory. C) Depiction of the figure series task (FS). On each trial participants were presented with a series of figures with one missing piece. Participants had to identify that missing piece from several presented options. This provides a measure of fluid intelligence.

possible accuracy score was 30 correct trials.

Statistical analyses

Pearson partial correlation analyses were conducted and correlation coefficients, r , and associated p -values are reported. Given known sex differences in MRE-derived measures of viscoelasticity (Arani et al., 2015; Sack et al., 2009), sex was included as a control variable. Correlations between viscoelastic measures (HC, OFC, PCC) and both cognitive measures (SR and FS tasks) were conducted. The significance of correlations was determined at $p < .05$, Bonferroni corrected, and indicated in the figures with an asterisk (*). Correlation coefficients for each structure-function pair were then compared by converting coefficients to z -scores, calculating the asymptotic covariance, and computing a z -statistic (Steiger, 1980). Given the nature of our hypotheses, one-tailed tests were considered when interpreting these data.

Results

Descriptive statistics after outlier removal (mean, standard deviation, minimum/maximum, skewness) for all dependent measures are reported in Table 1. Property values are reported as the mean across each region as defined by regional masks in native space. Regional masks varied in size with structure volume (average mask size: HC = 819 voxels; OFC = 3399 voxels; PCC = 801 voxels), and each region exhibited variance in ξ' (standard deviation over the regional mask: HC = 0.07; OFC = 0.11; PCC = 0.08). The Shapiro-Wilk test of normality indicated that while FS, OFC ξ' , and PCC ξ' measures were normally distributed, SR and HC ξ' measures were significantly skewed ($p < .02$ in both cases). Because of the skewed distribution, MAD methods were applied to detect outliers (Hampel, 1974; Leys et al., 2013). Six statistical outliers were detected (score greater than 3 times the MAD (Miller, 1991)): five due to memory performance and one due to HC ξ' . We note that the five participants removed for memory performance performed so poorly on the task that it is unlikely they were engaged in the task, and performed worse than bilateral hippocampal amnesic patients on the same task (Horecka et al., 2017).

The relationships among cognitive performance measures and among regional viscoelastic measures

SR-derived relational memory measures and FS-derived fluid intelligence measures were significantly correlated ($r = 0.43$, $p = .002$). Similarly, OFC ξ' was significantly correlated with both HC ξ' ($r = 0.28$, $p = .046$) and PCC ξ' ($r = 0.32$, $p = .023$). The relationship between HC ξ' and PCC ξ' was not significant ($r = 0.07$, $p = .631$).

The relationships between HC viscoelasticity and cognitive performance

Fig. 2 shows the relationship between HC ξ' and both relational memory (Fig. 2. top left) and fluid intelligence (Fig. 2. top right) task performance. HC ξ' significantly correlated with SR task performance ($r = 0.41$, $p = .002$), but not FS task performance ($r = 0.16$, $p = .270$). These data are consistent with our hypothesis that relational memory is tied to HC integrity, but not OFC integrity. HC μ did not significantly correlate with either SR task performance ($r = 0.12$, $p = .395$) or FS task performance ($r = 0.18$, $p = .192$). These data extend our previous work demonstrating the positive relationship between successful relational memory performance and HC ξ' (Schwarb et al., 2016; Schwarb et al., 2017) but not relational memory and viscoelasticity of another region associated with higher-order cognition (i.e., OFC).

The relationships between OFC viscoelasticity and cognitive performance

Fig. 2 shows the relationship between OFC ξ' and both relational memory (Fig. 2. bottom left) and fluid intelligence (Fig. 2. bottom right) task performance. Here, OFC ξ' significantly correlated with FS task

Table 1

Descriptive statistics of the study variables.

	Mean (SD)	Min/Max	Skewness
Cognitive Measures			
Spatial Reconstruction (SR)	3.39 (0.47)	2.0/4.3	−0.89
Figure Series (FS)	21.5 (4.7)	10/30	−0.38
MRE ξ' Measures			
HC ξ'	0.86 (0.03)	0.77/0.91	−0.58
OFC ξ'	0.80 (0.03)	0.71/0.87	−0.38
PCC ξ'	0.85 (0.02)	0.79/0.90	−0.11
MRE μ Measures			
HC μ [kPa]	2.96 (0.52)	1.90/4.31	0.29
OFC μ [kPa]	2.52 (0.25)	2.01/3.44	0.68
PCC μ [kPa]	2.87 (0.22)	2.43/3.44	0.02
Volume/Cortical Thickness Measures			
HC volume [cm ³]	9.01 (0.61)	7.72/10.33	−0.08
OFC thickness [mm]	2.65 (0.13)	2.42/2.93	0.57
PCC thickness [mm]	1.56 (0.12)	1.35/1.82	0.20

performance ($r = 0.42$, $p = .002$), but not SR task performance ($r = 0.12$, $p = .380$). OFC μ did not significantly correlate with either FS task performance ($r = 0.07$, $p = .619$) or SR task performance ($r = -0.13$, $p = .350$). To the best of our knowledge, these are the first data to show that MRE-derived structural measures are related to cognitive processes outside of memory.

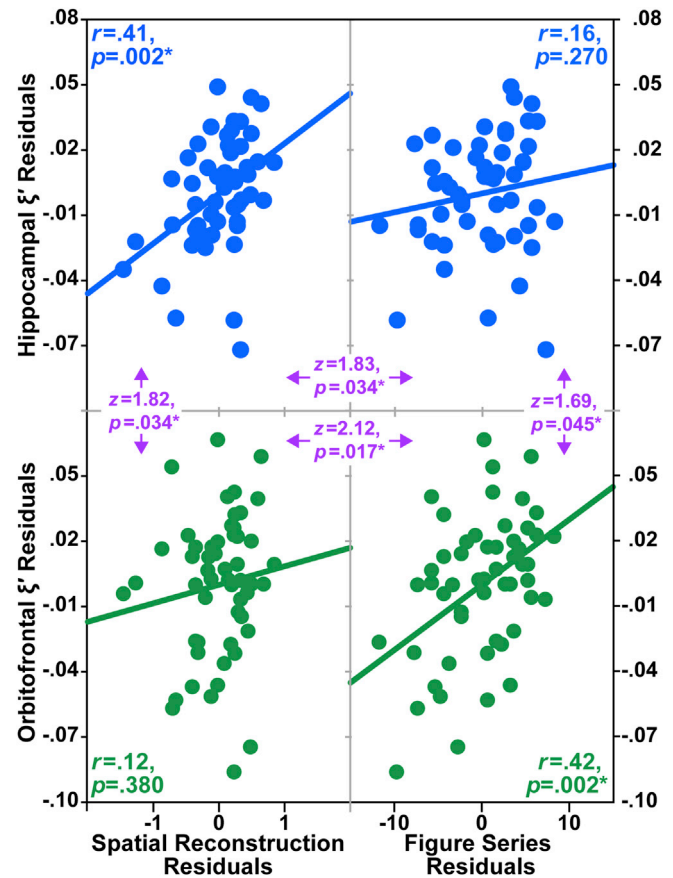


Fig. 2. Adjusted damping ratio (ξ') residuals plotted against behavioral performance residuals. Top left: Hippocampal ξ' residuals plotted against spatial reconstruction task residuals. Top right: Hippocampal ξ' residuals plotted against figure series task residuals. Bottom left: Orbitofrontal cortex ξ' residuals plotted against spatial reconstruction task residuals. Bottom right: Orbitofrontal cortex ξ' residuals plotted against figure series task residuals. Pearson correlation coefficients and associated p -values are included for each structure-function relationship. Comparisons of correlations indicated in purple with z -statistic and associated p -values. All significant relationships marked with *.

The relationships between PCC viscoelasticity and cognitive performance

We performed similar analyses comparing relational memory and fluid intelligence task performance to viscoelastic measures in the PCC, a control region that is not differentially involved in relational memory or fluid intelligence processes. Fig. 3 shows that PCC ξ' did not significantly correlate with either SR task performance ($r = 0.01$, $p = .963$) or FS task performance ($r = 0.04$, $p = .801$), as expected.

Double dissociation of structure-function relationships

As reported above, HC ξ' was significantly correlated with SR task performance, but not FS task performance. Importantly, these correlations also significantly differed from each other ($z = 1.83$, $p = .034$; Fig. 2. top). Similarly, OFC ξ' was significantly correlated with FS task performance, but not SR task performance. Again, these correlations significantly differed from each other ($z = 2.12$, $p = .017$; Fig. 2. bottom). Furthermore, the significant, positive correlation between SR task performance and HC ξ' was significantly greater than the nonsignificant correlation between SR and OFC ξ' ($z = 1.82$, $p = .034$; Fig. 2. left). Similarly, the significant, positive correlation between FS task performance and OFC ξ' was significantly greater than the nonsignificant correlation between FS and HC ξ' ($z = 1.69$, $p = .045$; Fig. 2. right). This double dissociation highlights the relationship between HC integrity to relational memory performance, but not fluid intelligence performance, and the relationship between OFC integrity to fluid intelligence performance, but not relational memory performance among healthy, young adults.

The relationships between regional volume or thickness and cognitive performance

Structure-function analyses were also performed considering volume (HC) and cortical thickness (OFC and PCC) measures. HC volume did not correlate significantly with SR task performance ($r = 0.07$; $p = .632$), as previously reported (Schwarb et al., 2017), nor with the FS task ($r = 0.16$; $p = .244$). OFC thickness did not correlate significantly with performance on either the FS task ($r = -0.08$; $p = .574$) or the SR task ($r = -0.19$; $p = .163$). PCC thickness also did not correlate significantly with performance on either the FS task ($r = 0.134$; $p = .331$) or the SR task ($r = -0.01$; $p = .956$).

Discussion

Building on the previous successes in using MRE to examine the

relationship between HC viscoelasticity and memory performance (Sandroff et al., 2017; Schwarb et al., 2016, 2017), this work represents the first examination of an MRE-derived dissociable structure-function relationship in the human brain. We report a positive correlation between viscoelasticity of the OFC and performance on a fluid intelligence task in our sample of healthy young adults. Similar to our previous observations in the HC, we find that higher OFC ξ' , indicating more elastic tissue behavior, is related to better task performance. We also did not observe a significant relationship between OFC μ , again similar to our previous findings in the HC (Schwarb et al., 2016). However, in other populations with compromised tissue integrity, such as in aging (Arani et al., 2015), we would expect to find effects with μ . Finally, the lack of relationships between task performance and OFC thickness, despite the positive relationship with OFC ξ' , further enhances the idea that MRE measures are potentially more sensitive to microstructural tissue health than thickness/volume measures, especially in young adult populations. We also note that these findings persist even if we do not remove statistical outliers and instead perform nonparametric correlations.

The finding that OFC integrity is related to fluid intelligence task performance complements previous work from neuropsychological patients with frontal lobe damage (Barbey et al., 2013; Woolgar et al., 2010), functional neuroimaging studies of regional activation accompanying performance on FS fluid intelligence tests (Duncan et al., 2000; Masunaga et al., 2008), and aging work comparing OFC volume to successful fluid intelligence performance (Gong et al., 2005; Raz et al., 2008). These data are encouraging as they suggest that MRE measures of microstructural integrity are sensitive enough to detect cognition-relevant structural differences even among healthy young adults (Schwarb et al., 2016; Schwarb et al., 2017); however, a single dissociation is not sufficient to demonstrate the specificity of this tool for mapping cognitive function, but rather a double dissociation is essential for specifically associating given regions with given functions (Fama and Sullivan, 2014). For this purpose, we consider our previously reported HC-relational memory relationship (Schwarb et al., 2016; Schwarb et al., 2017) as a comparison structure-function relationship for the novel OFC-fluid intelligence finding reported here. A subset of these data have been previously reported (Schwarb et al., 2017), however, the current data report a novel overall relational memory accuracy measure instead of the previously reported individual error measures (note that the current findings are similar if we instead consider the previously reported error metrics). The HC and the OFC are structurally connected (Heide Von Der et al., 2013; Sasson et al., 2013) and HC-OFC interactions have been implicated in supporting both mnemonic processing (Preston and Eichenbaum, 2013; Zeithamova and Preston, 2010) as well as fluid intelligence (Kane and Engle, 2002). Although highly interconnected structures, independently, the HC is critical for relational memory processing (Cohen and Eichenbaum, 1993; Eichenbaum and Cohen, 2001) and not generally implicated in fluid intelligence processes among healthy, young adults (Reuben et al., 2011), thus making it an optimal comparison structure.

The data reported here demonstrate a significant double dissociation suggesting that MRE is a sensitive tool that can make a unique contribution in the effort to map cognitive processes in the brain, particularly among healthy, young adults for whom other structural measures, such as volume, are not typically informative to cognition. OFC viscoelastic measures showed a significant positive relationship with FS task performance, but not SR task performance; and these correlations significantly differed. Furthermore, HC viscoelastic measures showed a significant positive relationship with SR task performance, but not FS task performance; and, again, these correlations significantly differed. These data, of course, should not be interpreted as supporting a modular or fractionation view of cognitive function in the brain (Fama and Sullivan, 2014; Poldrack, 2010; Sarter et al., 1996). Indeed, these data do not suggest that the HC and OFC are the only structures necessary (or even critical) to support relational memory and fluid intelligence processes, respectively. Rather, these data suggest that there are individual

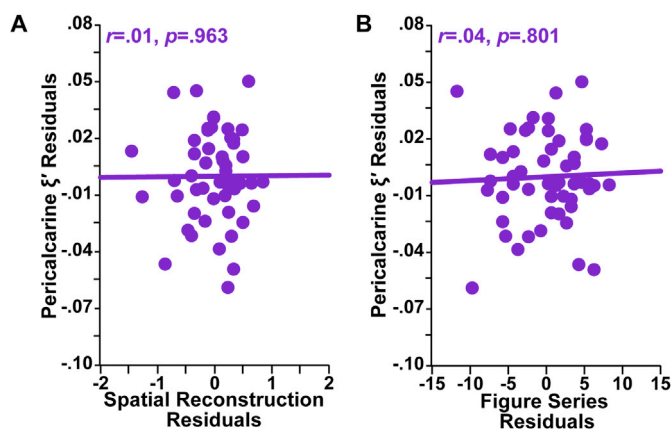


Fig. 3. Pericalcarine cortex (PCC) adjusted damping ratio (ξ') residuals plotted against A) spatial reconstruction task residuals and B) figure series task residuals. Pearson correlation coefficients and associated p -values are included for each structure-function relationship.

differences in the microstructure of these regions that are sensitive to variability in performance on dissociable cognitive tasks. To the best of our knowledge, this is the first report of MRE-derived dissociable structure-function relationships in the human brain. These data promote the use of MRE as an effective and sensitive tool to study the neuroanatomy of cognition across cognitive domains.

Interestingly, the MRE measures showed correlation between regions (i.e. HC and OFC, OFC and PCC, but not HC and PCC). Similar findings from brain MRE have been reported previously (Johnson et al., 2016; Murphy et al., 2013), and suggest that some of the regional variability is driven by differences in global viscoelasticity, though with regional measures differentially affected by aging and disease (Arani et al., 2015; Murphy et al., 2016) or differentially supporting cognitive processes, as reported in this work. Future work employing MRE in human brain mapping will enable a more complete assessment of the sensitivity and specificity of regional viscoelastic measures as they relate to cognitive function.

In addition to the theoretical contributions to the study of cognition, this work also represents a technical extension of brain MRE investigations to gray matter of the cortex, which is particularly challenging for achieving reliable property estimates with MRE. The cortex is thin, surrounded by CSF, and the mechanical behavior at sulci likely violates the model of tissue as a semi-infinite medium used in MRE, all of which are expected to reduce accuracy and increase uncertainty of cortical property measures. Despite several brain MRE studies that reported differences between white matter and cortical gray matter (Clayton et al., 2012; Johnson et al., 2013a; Zhang et al., 2011), which were consistent with *ex vivo* studies of animal brain mechanics (van Dommelen et al., 2010), in recent years reliable measures of cortical properties have been treated as a goal for future developments in inversion algorithms and image resolution, including the extension to ultrahigh-field 7T MRI scanners (Braun et al., 2014).

To obtain the OFC measures described in this work, we applied the same approach as previously developed for subcortical gray matter, specifically the use of an imaging sequence capable of 1.6 mm imaging resolution (Johnson et al., 2014) and inversion with NLI and SPR (McGarry et al., 2013). We previously demonstrated that both higher resolution and the use of SPR improved the reliability of MRE measures in subcortical structures (Johnson et al., 2016), including the HC, and we similarly estimated the repeatability of the OFC MRE measures from the same eight repeated exams on a single subject. We found that the coefficient of variation ($CV = \text{st. dev.}/\text{mean}$) for ξ of the OFC was 6.7%, computed using the average ξ in the OFC region for each of the eight exams, which is comparable to the CVs of ξ in subcortical structures we reported previously (Johnson et al., 2016). This provides confidence in our OFC MRE measurements, and supports the assertion that these investigations yield useful and meaningful outcomes. However, as in other *in vivo* brain MRE studies, we are not able to directly validate cortical MRE through other independent assessments, and it is likely that further technical developments will improve both the accuracy and precision of cortical MRE measures.

The results presented in this paper are from an ROI-based analysis of MRE data, which is the standard analysis approach in the brain MRE literature (Hiscox et al., 2016). ROIs were chosen based on expected structure-function relationships (and lack of relationships in case of the PCC control region), and realistic volume masks were created in native space using subject-specific regional segmentations of anatomical images that were also used as spatial priors during inversion (McGarry et al., 2013). Both the repeatability results presented above and our previous work (Johnson et al., 2016) demonstrate that this type of analysis provides reliable estimate of brain tissue mechanical properties. Future studies that instead adopt a voxel-based analysis approach have the potential to more completely explore contributions of mechanical properties throughout the entire brain to performance on cognitive tasks. Such analyses are currently lacking in the brain MRE field, and are outside the scope of this current work, though they should be considered in future

MRE brain mapping studies. Such studies should also critically consider how MRE data characteristics, including resolution and uncertainty after transformation to standard space, affect statistical parametric maps and inform the proper analysis techniques.

One of the major limitations in the interpretation of brain MRE results is the ambiguity surrounding the biological basis of the observed viscoelastic effects. The damping ratio, which describes relative tissue viscosity and is similar to mechanical phase angle often reported in brain MRE (Lipp et al., 2013; Schregel et al., 2012), is expected to relate to the microstructural organization of tissue (Sack et al., 2013). We previously hypothesized that higher HC ξ' measures may reflect differences associated with neurogenesis (Schwarb et al., 2017), which is supported by animal MRE studies that showed viscoelastic effects related to neurogenesis and neuronal density (Hain et al., 2016; Klein et al., 2014; Munder et al., 2018). As we extend our measurements beyond the HC to the OFC, the biological mechanism that describes the positive relationship between ξ' and behavioral performance in both subcortical and cortical gray matter needs to be seriously considered. While adult neurogenesis is unique to the HC and olfactory bulb, structural changes in other regions, including the PFC, have been reported, particularly following exercise interventions, indicating that other mechanisms are at work (Erickson et al., 2014). Additional research is required to solidify the neurobiological basis of the MRE signal, however, there are several candidate mechanisms to consider. In addition to the evidence supporting neuronal density, microvasculature may also contribute to the MRE properties (Jugé et al., 2015). Hetzer and colleagues suggested that perfusion may alter stiffness in subcortical structures (Hetzer et al., 2018), though they did not report viscous tissue properties, and thus more work is needed to consider our results as they may be related to perfusion. The use of additional quantitative imaging techniques, which are complementary to MRE and with shared sensitivity to elements of neural tissue microstructure, such as neurite orientation dispersion and density imaging (NODDI) (Zhang et al., 2012) and quantitative susceptibility mapping (QSM) (Li et al., 2011), may help elucidate the mechanisms underpinning the observed structure-function relationships reported in this work.

Conclusions

The discovery of a structure-function relationship in the HC observable with MRE opened a realm of possibilities for examining the brain through the sensitive measures of neural tissue mechanics. It followed that other structure-function relationships could be similarly probed with brain MRE, and, in this work, we successfully use MRE to probe OFC viscoelasticity and how it relates to performance on a fluid intelligence task. This provides another neural substrate where the sensitivity of the MRE contrast can be used to examine tissue health in response to intervention or disease with a link to the functional outcomes. We also provide evidence to support the specificity of MRE measures through the first observation of a double dissociation in mechanical structure and function. These data highlight the existence of detectable microstructural variability that is meaningful to cognitive performance even among healthy young adults and that MRE may provide an effective tool for probing structure-function associations for early disease detection, staging decline, or monitoring recovery with rehabilitation. Ultimately, this finding supports the use of MRE beyond the HC and OFC to all subcortical and cortical regions in order to mechanically map the human brain.

Acknowledgments

The research is based upon work supported by the Office of the Director of National Intelligence (ODNI), Intelligence Advanced Research Projects Activity (IARPA), via Contract 2014-13121700004 to the University of Illinois at Urbana-Champaign. The views and conclusions contained herein are those of the authors and should not be interpreted

as necessarily representing the official policies or endorsements, either expressed or implied, of the ODNI, IARPA, or the U.S. Government. The U.S. Government is authorized to reproduce and distribute reprints for Governmental purposes notwithstanding any copyright annotation thereon. This research is additionally part of the Blue Waters sustained-petascale computing project, which is supported by the National Science Foundation (awards OCI-0725070 and ACI-1238993) and the state of Illinois. Blue Waters is a joint effort of the University of Illinois at Urbana-Champaign and its National Center for Supercomputing Applications. MRE data acquisition and analysis was further supported by NIH/NIBIB grants R01-EB018320 and R01-001981. We would also like to thank Patricia Jones (project manager), Courtney Allen (project coordinator), Ginger Reeser (project coordinator), and the entire INSIGHT staff for their commitment and dedication to the success of this work. This work was carried out in part at the Biomedical Imaging Center of the Beckman Institute for Advanced Science and Technology at the University of Illinois.

References

- Arani, A., Murphy, M.C., Glaser, K.J., Manduca, A., Lake, D.S., Kruse, S.A., Jack, C.R., Ehman, R.L., Huston, J., 2015. Measuring the effects of aging and sex on regional brain stiffness with MR elastography in healthy older adults. *NeuroImage* 111, 59–64.
- Barbey, A.K., Colom, R., Paul, E.J., Grafman, J., 2013. Architecture of fluid intelligence and working memory revealed by lesion mapping. *Brain Struct. Funct.* 219, 485–494.
- Bigler, E.D., 2009. Hans-Lukas Teuber and “The riddle of frontal lobe function in man” as published in the frontal granular cortex and behavior (1964). *Neuropsychol. Rev.* 19, 9–24.
- Braun, J., Guo, J., Lutzendorf, R., Papazoglou, S., Hirsch, S., Sack, I., Bernarding, J., 2014. High-resolution mechanical imaging of the human brain by three-dimensional multifrequency magnetic resonance elastography at 7T. *NeuroImage* 90, 308–314.
- Buckner, R.L., Head, D., Parker, J., Fotenos, A.F., Marcus, D., Morris, J.C., Snyder, A.Z., 2004. A unified approach for morphometric and functional data analysis in young, old, and demented adults using automated atlas-based head size normalization: reliability and validation against manual measurement of total intracranial volume. *NeuroImage* 23, 724–738.
- Burkard, R., Dell’Amico, M., Martello, S., 2012. Assignment Problems. Society for Industrial and Applied Mathematics, Philadelphia, PA.
- Carroll, J.B., 1993. Human Cognitive Abilities: a Survey of Factor-analytic Studies.
- Cattell, R.B., 1971. Abilities: Their Structure, Growth, and Action.
- Clayton, E.H., Genin, G.M., Bayly, P.V., 2012. Transmission, attenuation and reflection of shear waves in the human brain. *J. R. Soc. Interface* 9, 2899–2910.
- Cohen, N.J., Eichenbaum, H., 1993. Memory, Amnesia, and the Hippocampal System. MIT Press.
- Daugherty, A.M., Zwilling, C.M., Paul, E.J., Sherpa, N., Allen, C.M., Kramer, A.F., Hillman, C.H., Cohen, N.J., Barbey, A.K., 2018. Multi-modal fitness and cognitive training to enhance fluid intelligence. *Intelligence* 66, 32–43.
- de Abreu, P.M.J.E., Conway, A.R.A., Gathercole, S.E., 2010. Working memory and fluid intelligence in young children. *Intelligence* 38, 552–561.
- Desikan, R.S., Segonne, F., Fischl, B., Quinn, B.T., Dickerson, B.C., Blacker, D., Buckner, R.L., Dale, A.M., Maguire, R.P., Hyman, B.T., Albert, M.S., Killiany, R.J., 2006. An automated labeling system for subdividing the human cerebral cortex on MRI scans into gyral based regions of interest. *NeuroImage* 31, 968–980.
- Duncan, J., Burgess, P., Emslie, H., 1995. Fluid intelligence after frontal-lobe lesions. *Neuropsychologia* 33, 261–268.
- Duncan, J., Seitz, R.J., Kolodny, J., Bor, D., Herzog, H., Ahmed, A., Newell, F.N., Emslie, H., 2000. A neural basis for general intelligence. *Science* 289, 457–460.
- Eichenbaum, H., Cohen, N.J., 2001. From Conditioning to Conscious Recollection: Memory Systems of the Brain. Oxford University Press.
- Erickson, K.I., Leckie, R.L., Weinstein, A.M., 2014. Physical activity, fitness, and gray matter volume. *Neurobiol. Aging* 35 (Suppl. 2), S20–S28.
- Erickson, K.I., Prakash, R.S., Voss, M.W., Chaddock, L., Hu, L., Morris, K.S., White, S.M., Wójcicki, T.R., McAuley, E., Kramer, A.F., 2009. Aerobic fitness is associated with hippocampal volume in elderly humans. *Hippocampus* 19, 1030–1039.
- Fama, R., Sullivan, E.V., 2014. Methods of association and dissociation for establishing selective brain-behavior relations. In: Sullivan, E.V., Pfefferbaum, A. (Eds.), *Handbook of Clinical Neurology*, vol 125. Alcohol and the Nervous System. Elsevier, pp. 175–181. Vol. 125.
- Fischl, B., 2012. FreeSurfer. *NeuroImage* 62, 774–781.
- Fischl, B., Dale, A.M., 2000. Measuring the thickness of the human cerebral cortex from magnetic resonance images. *P Natl. Acad. Sci. USA* 97, 11050–11055.
- Fischl, B., Salat, D.H., Busa, E., Albert, M.S., Dieterich, M., Haselgrove, C., van der Kouwe, A., Killiany, R., Kennedy, D.N., Klaveness, S., Montillo, A., Makris, N., Rosen, B., Dale, A.M., 2002. Whole brain segmentation: automated labeling of neuroanatomical structures in the human brain. *Neuron* 33, 341–355.
- Freedman, M., Alexander, M.P., Naeser, M.A., 1984. Anatomic basis of transcortical motor aphasia. *Neurology* 34, 409–417.
- Freimann, F.B., Müller, S., Streitberger, K.-J., Guo, J., Rot, S., Ghori, A., Vajkoczy, P., Reiter, R., Sack, I., Braun, J., 2013. MR elastography in a murine stroke model reveals correlation of macroscopic viscoelastic properties of the brain with neuronal density. *NMR Biomed.* 26, 1534–1539.
- Funai, A.K., Fessler, J.A., Yeo, D.T.B., Olafsson, V.T., Noll, D.C., 2008. Regularized field map estimation in MRI. *IEEE T Med. Imag.* 27, 1484–1494.
- Glover, G.H., 1999. Simple analytic spiral K-Space algorithm. *Magn. Reson. Med.* 42, 412–415.
- Gong, Q.-Y., Sluming, V., Mayes, A., Keller, S., Barrick, T., Cezayirli, E., Roberts, N., 2005. Voxel-based morphometry and stereology provide convergent evidence of the importance of medial prefrontal cortex for fluid intelligence in healthy adults. *NeuroImage* 25, 1175–1186.
- Hain, E.G., Klein, C., Munder, T., Braun, J., Riek, K., Mueller, S., Sack, I., Steiner, B., 2016. Dopaminergic neurodegeneration in the mouse is associated with decrease of viscoelasticity of substantia nigra tissue. *PLoS One* 11, e0161179.
- Hampel, F.R., 1974. The influence curve and its role in robust estimation. *J. Am. Stat. Assoc.* 69, 383–393.
- Heide Von Der, R.J., Skipper, L.M., Klobusicky, E., Olson, I.R., 2013. Dissecting the uncinate fasciculus: disorders, controversies and a hypothesis. *Brain* 136, 1692–1707.
- Hetzer, S., Birr, P., Fehlnner, A., Hirsch, S., Dittmann, F., Barnhill, E., Braun, J., Sack, I., 2018. Perfusion alters stiffness of deep gray matter. *J. Cerebr. Blood Flow Metabol.* 38, 116–125.
- Hiscox, L.V., Johnson, C.L., Barnhill, E., McGarry, M.D.J., Huston, J., van Beek, E.J.R., Starr, J.M., Roberts, N., 2016. Magnetic resonance elastography (MRE) of the human brain: technique, findings and clinical applications. *Phys. Med. Biol.* 61, R401–R437.
- Horecka, K.M., Dulas, M.R., Schwarb, H., Lucas, H.D., Duff, M.C., Cohen, N.J., 2017. Reconstructing relational information. *Hippocampus*. <https://doi.org/10.1002/hipo.22819> in press.
- Hughes, J.D., Fattahi, N., Van Gompel, J., Arani, A., Ehman, R.L., Huston, J., 2016. Magnetic resonance elastography detects tumoral consistency in pituitary macroadenomas. *Pituitary* 19, 286–292.
- Hughes, J.D., Fattahi, N., Van Gompel, J., Arani, A., Meyer, F.B., Lanzino, G., Link, M.J., Ehman, R.L., Huston, J., 2015. Higher-resolution magnetic resonance elastography in meningiomas to determine intratumoral consistency. *Neurosurgery* 77, 653–659.
- Huston, J., Murphy, M.C., Boeve, B.F., Fattahi, N., Arani, A., Glaser, K.J., Manduca, A., Jones, D.T., Ehman, R.L., 2016. Magnetic resonance elastography of frontotemporal dementia. *J. Magn. Reson. Imag.* 43, 474–478.
- Jaeggi, S.M., Buschkuhl, M., Jonides, J., Perrig, W.J., 2008. Improving fluid intelligence with training on working memory. *P Natl. Acad. Sci. USA* 105, 6829–6833.
- Jenkinson, M., 2003. Fast, automated, N-dimensional phase-unwrapping algorithm. *Magn. Reson. Med.* 49, 193–197.
- Jenkinson, M., Bannister, P.R., Brady, M., Smith, S.M., 2002. Improved optimization for the robust and accurate linear registration and motion correction of brain images. *NeuroImage* 17, 825–841.
- Jenkinson, M., Beckmann, C.F., Behrens, T.E.J., Woolrich, M.W., Smith, S.M., 2012. FSL. *NeuroImage* 62, 782–790.
- Johnson, C.L., Holtrop, J.L., McGarry, M.D.J., Weaver, J.B., Paulsen, K.D., Georgiadis, J.G., Sutton, B.P., 2014. 3D multislab, multishot acquisition for fast, whole-brain MR elastography with high signal-to-noise efficiency. *Magn. Reson. Med.* 71, 477–485.
- Johnson, C.L., McGarry, M.D.J., Gharibans, A.A., Weaver, J.B., Paulsen, K.D., Wang, H., Olivero, W.C., Sutton, B.P., Georgiadis, J.G., 2013a. Local mechanical properties of white matter structures in the human brain. *NeuroImage* 79, 145–152.
- Johnson, C.L., McGarry, M.D.J., Van Houten, E.E.W., Weaver, J.B., Paulsen, K.D., Sutton, B.P., Georgiadis, J.G., 2013b. Magnetic resonance elastography of the brain using multishot spiral readouts with self-navigated motion correction. *Magn. Reson. Med.* 70, 404–412.
- Johnson, C.L., Schwarb, H., McGarry, M.D.J., Anderson, A.T., Huesmann, G.R., Sutton, B.P., Cohen, N.J., 2016. Viscoelasticity of subcortical gray matter structures. *Hum. Brain Mapp.* 37, 4221–4233.
- Johnson, C.L., Telzer, E.H., 2017. Magnetic resonance elastography for examining developmental changes in the mechanical properties of the brain. *Dev. Cogn. Neurosci.* <https://doi.org/10.1016/j.dcn.2017.08.010> in press.
- Jugé, L., Petiet, A., Lambert, S.A., Nicole, P., Chatelin, S., Vilgrain, V., van Beers, B.E., Bilston, L.E., Sinkus, R., 2015. Microvasculature alters the dispersion properties of shear waves—a multi-frequency MR elastography study. *NMR Biomed.* 28, 1763–1771.
- Kane, M.J., Engle, R.W., 2002. The role of prefrontal cortex in working-memory capacity, executive attention, and general fluid intelligence: an individual-differences perspective. *Psychonomic Bull. Rev.* 9, 637–671.
- Klein, C., Hain, E.G., Braun, J., Riek, K., Mueller, S., Steiner, B., Sack, I., 2014. Enhanced adult neurogenesis increases brain stiffness: in vivo magnetic resonance elastography in a mouse model of dopamine depletion. *PLoS One* 9, e92582.
- Lays, C., Ley, C., Klein, O., Bernard, P., Licata, L., 2013. Detecting outliers: do not use standard deviation around the mean, use absolute deviation around the median. *J. Exp. Soc. Psychol.* 49, 764–766.
- Li, W., Wu, B., Liu, C., 2011. Quantitative susceptibility mapping of human brain reflects spatial variation in tissue composition. *NeuroImage* 55, 1645–1656.
- Lipp, A., Trbojevic, R., Paul, F., Fehlnner, A., Hirsch, S., Scheel, M., Noack, C., Braun, J., Sack, I., 2013. Cerebral magnetic resonance elastography in supranuclear palsy and idiopathic Parkinson's disease. *NeuroImage Clin.* 3, 381–387.
- Manduca, A., Oliphant, T.E., Dresner, M.A., Mahowald, J.L., Kruse, S.A., Amromin, E., Felmlee, J.P., Greenleaf, J.F., Ehman, R.L., 2001. Magnetic resonance elastography: non-invasive mapping of tissue elasticity. *Med. Image Anal.* 5, 237–254.
- Masunaga, H., Kawashima, R., Horn, J.L., Sassa, Y., Sekiguchi, A., 2008. Neural substrates of the Topology Test to measure fluid reasoning: an fMRI study. *Intelligence* 36, 607–615.

- McGarry, M.D.J., Johnson, C.L., Sutton, B.P., Van Houten, E.E.W., Georgiadis, J.G., Weaver, J.B., Paulsen, K.D., 2013. Including spatial information in nonlinear inversion MR elastography using soft prior regularization. *IEEE T Med. Imag.* 32, 1901–1909.
- McGarry, M.D.J., Van Houten, E.E.W., 2008. Use of a Rayleigh damping model in elastography. *Med. Biol. Eng. Comput.* 46, 759–766.
- McGarry, M.D.J., Van Houten, E.E.W., Johnson, C.L., Georgiadis, J.G., Sutton, B.P., Weaver, J.B., Paulsen, K.D., 2012. Multiresolution MR elastography using nonlinear inversion. *Med. Phys.* 39, 6388–6396.
- Miller, J., 1991. Reaction time analysis with outlier exclusion: bias varies with sample size. *Q. J. Exp. Psychol.* 43, 907–912.
- Monti, J.M., Cooke, G.E., Watson, P.D., Voss, M.W., Kramer, A.F., Cohen, N.J., 2015. Relating hippocampus to relational memory processing across domains and delays. *J. Cogn. Neurosci.* 27, 234–245.
- Munder, T., Pfeffer, A., Schreyer, S., Guo, J., Braun, J., Sack, I., Steiner, B., Klein, C., 2018. MR elastography detection of early viscoelastic response of the murine hippocampus to amyloid β accumulation and neuronal cell loss due to Alzheimer's disease. *J. Magn. Reson. Imag.* 47, 105–114.
- Murphy, M.C., Huston, J., Jack, C.R., Glaser, K.J., Senjem, M.L., Chen, J., Manduca, A., Felmlee, J.P., Ehman, R.L., 2013. Measuring the characteristic topography of brain stiffness with magnetic resonance elastography. *PLoS One* 8, e81668.
- Murphy, M.C., Jones, D.T., Jack, C.R., Glaser, K.J., Senjem, M.L., Manduca, A., Felmlee, J.P., Carter, R.E., Ehman, R.L., Huston, J., 2016. Regional brain stiffness changes across the Alzheimer's disease spectrum. *NeuroImage Clin.* 10, 283–290.
- Muthupillai, R., Lomas, D.J., Rossman, P.J., Greenleaf, J.F., Manduca, A., Ehman, R.L., 1995. Magnetic resonance elastography by direct visualization of propagating acoustic strain waves. *Science* 269, 1854–1857.
- Poldrack, R.A., 2010. Mapping Mental function to brain structure: how can cognitive neuroimaging succeed? *Perspect. Psychol. Sci.* 5, 753–761.
- Preston, A.R., Eichenbaum, H., 2013. Interplay of hippocampus and prefrontal cortex in memory. *Curr. Biol.* 23, R764–R773.
- Pruessmann, K.P., Weiger, M., Börnert, P., Boesiger, P., 2001. Advances in sensitivity encoding with arbitrary k-space trajectories. *Magn. Reson. Med.* 46, 638–651.
- Raz, N., 2000. Aging of the brain and its impact on cognitive performance: integration of structural and functional findings. In: Craik, F.I.M., Salthouse, T.A. (Eds.), *Handbook of Aging and Cognition*, pp. 1–90.
- Raz, N., Lindenberger, U., Ghisletta, P., Rodrigue, K.M., Kennedy, K.M., Acker, J.D., 2008. Neuroanatomical correlates of fluid intelligence in healthy adults and persons with vascular risk factors. *Cerebr. Cortex* 18, 718–726.
- Raz, N., Lindenberger, U., Rodrigue, K.M., Kennedy, K.M., Head, D., Williamson, A., Dahle, C., Gerstorf, D., Acker, J.D., 2005. Regional brain changes in aging healthy adults: general trends, individual differences and modifiers. *Cerebr. Cortex* 15, 1676–1689.
- Reuben, A., Brickman, A.M., Muraskin, J., Steffener, J., Stern, Y., 2011. Hippocampal atrophy relates to fluid intelligence decline in the elderly. *J. Int. Neuropsychol. Soc.* 17, 56–61.
- Riek, K., Millward, J.M., Hamann, I., Mueller, S., Pfueller, C.F., Paul, F., Braun, J., Infante-Duarte, C., Sack, I., 2012. Magnetic resonance elastography reveals altered brain viscoelasticity in experimental autoimmune encephalomyelitis. *Neuroimage Clin.* 1, 81–90.
- Romano, A.J., Guo, J., Prokscha, T., Meyer, T., Hirsch, S., Braun, J., Sack, I., Scheel, M., 2014. In vivo waveguide elastography: effects of neurodegeneration in patients with amyotrophic lateral sclerosis. *Magn. Reson. Med.* 72, 1755–1761.
- Sack, I., Beierbach, B., Wuerfel, J., Klatt, D., Hamhaber, U., Papazoglou, S., Martus, P., Braun, J., 2009. The impact of aging and gender on brain viscoelasticity. *Neuroimage* 46, 652–657.
- Sack, I., Jöhrens, K., Wuerfel, J., Braun, J., 2013. Structure-sensitive elastography: on the viscoelastic power law behavior of in vivo human tissue in health and disease. *Soft Matter* 9, 5672–5680.
- Sack, I., Streitberger, K.-J., Krefting, D., Paul, F., Braun, J., 2011. The influence of physiological aging and atrophy on brain viscoelastic properties in humans. *PLoS One* 6, e23451.
- Sandrock, B.M., Johnson, C.L., Motl, R.W., 2017. Exercise training effects on memory and hippocampal viscoelasticity in multiple sclerosis: a novel application of magnetic resonance elastography. *Neuroradiology* 59, 61–67.
- Sarter, M., Berntson, G.G., Cacioppo, J.T., 1996. Brain imaging and cognitive neuroscience. Toward strong inference in attributing function to structure. *Am. Psychol.* 51, 13–21.
- Sasson, E., Doniger, G.M., Pasternak, O., Tarrasch, R., Assaf, Y., 2013. White matter correlates of cognitive domains in normal aging with diffusion tensor imaging. *Front. Neurosci.* 7, 32.
- Schregel, K., Wuerfel, E., Garteiser, P., Gemeinhardt, I., Prozorovski, T., Aktas, O., Merz, H., Petersen, D., Wuerfel, J., Sinkus, R., 2012. Demyelination reduces brain parenchymal stiffness quantified in vivo by magnetic resonance elastography. *P Natl. Acad. Sci. USA* 109, 6650–6655.
- Schwarb, H., Johnson, C.L., Daugherty, A.M., Hillman, C.H., Kramer, A.F., Cohen, N.J., Barbey, A.K., 2017. Aerobic fitness, hippocampal viscoelasticity, and relational memory performance. *Neuroimage* 153, 179–188.
- Schwarb, H., Johnson, C.L., McGarry, M.D.J., Cohen, N.J., 2016. Medial temporal lobe viscoelasticity and relational memory performance. *Neuroimage* 132, 534–541.
- Steiger, J.H., 1980. Tests for comparing elements of a correlation matrix. *Psychol. Bull.* 87, 245–251.
- Streitberger, K.-J., Sack, I., Krefting, D., Pfüller, C., Braun, J., Paul, F., Wuerfel, J., 2012. Brain viscoelasticity alteration in chronic-progressive multiple sclerosis. *PLoS One* 7, e29888.
- Sutton, B.P., Noll, D.C., Fessler, J.A., 2003. Fast, iterative image reconstruction for MRI in the presence of field inhomogeneities. *IEEE T Med. Imag.* 22, 178–188.
- Teuber, H.-L., 1955. Physiological psychology. *Annu. Rev. Psychol.* 6, 267–296.
- Tranel, D., Manzel, K., Anderson, S.W., 2008. Is the prefrontal cortex important for fluid intelligence? A neuropsychological study using matrix reasoning. *Clin. Neuropsychol.* 22, 242–261.
- van Dommelen, J.A.W., van der Sande, T.P.J., Hrapko, M., Peters, G.W.M., 2010. Mechanical properties of brain tissue by indentation: interregional variation. *J. Mech. Behav. Biomed. Mater.* 3, 158–166.
- Winkler, A.M., Kochunov, P., Blangero, J., Almasy, L., Zilles, K., Fox, P.T., Duggirala, R., Glahn, D.C., 2010. Cortical thickness or grey matter volume? The importance of selecting the phenotype for imaging genetics studies. *Neuroimage* 53, 1135–1146.
- Woolgar, A., Parr, A., Cusack, R., Thompson, R., Nimmo-Smith, I., Torralva, T., Roca, M., Antoun, N., Manes, F., Duncan, J., 2010. Fluid intelligence loss linked to restricted regions of damage within frontal and parietal cortex. *P Natl. Acad. Sci. USA* 107, 14899–14902.
- Zeithamova, D., Preston, A.R., 2010. Flexible memories: differential roles for medial temporal lobe and prefrontal cortex in cross-episode binding. *J. Neurosci.* 30, 14676–14684.
- Zhang, H., Schneider, T., Wheeler-Kingshott, C.A., Alexander, D.C., 2012. NODDI: practical in vivo neurite orientation dispersion and density imaging of the human brain. *Neuroimage* 61, 1000–1016.
- Zhang, J., Green, M.A., Sinkus, R., Bilston, L.E., 2011. Viscoelastic properties of human cerebellum using magnetic resonance elastography. *J. Biomech.* 44, 1909–1913.